Available online at www.sciencedirect.com
SCIENCE DIRECT®
International Journal of Heat and Mass Transfer 47 (2004) 4637–4648
International Journal of HEAT and MASS TRANSFER
www.elsevier.com/locate/ijhmt

Nucleate boiling of two and three-component mixtures

Yasunobu Fujita *, Masayuki Tsutsui

Department of Mechanical Engineering Science, Kyushu University, 6-10-1 Hakozaki, Higashi-ku, Fukuoka 812-8581, Japan

Received 18 April 2003; received in revised form 13 June 2003

Abstract

For three pure fluids and their two- and three-component mixtures, heat transfer coefficients were measured in nucleate pool boiling on the upward facing copper surface of 40 mm diameter. The more-, moderate- and less-volatile components in mixtures are refrigerants R-134a, R-142b and R-123, respectively. Heat transfer coefficients of mixtures were less than the interpolated heat transfer coefficients between pure components, with more reduction at higher heat flux. Two correlations originally developed for two-component mixtures by Thome and Shakir and by Fujita and Tsutsui reproduced well the measured heat transfer coefficients of three- as well as two-component mixtures. This result implies that the boiling range included in the correlations accounts for heat transfer reduction in mixture boiling.

Keywords: Pool boiling; Heat transfer; Mixtures; Two- and three-components; Correlation

1. Introduction

Boiling heat transfer has been intensively investigated and our knowledge on heat transfer mechanism is made broader. But it is not an easy task to predict boiling heat transfer coefficient even for single-component pure fluids. This situation becomes more serious for multi-component mixtures. Many previous investigations of two-component mixtures have revealed that heat transfer coefficients are reduced in comparison with either the predicted values assuming the mixture as pure fluid of the same physical properties or the interpolated values between mixture components. For the reduction of heat transfer coefficient various mechanisms [1–6] are proposed, while it is not yet made clear which mechanism is responsible for heat transfer reduction in mixture boiling.

In designing or evaluating heat exchanger or phase change equipment employing mixtures as working fluid it is highly required to predict boiling heat transfer coefficient of given mixtures with tolerable errors. For this purpose several empirical or semi-empirical correlations [4,5,7–14] were proposed in the literature. However the validation of such available correlations were assessed mostly for two-component mixtures and their pervasive applicability to three- or more than three-component mixtures is not fully investigated and thus their validity remains unclear. Even for three-component mixtures, available heat transfer data are very limited [7,15,16] and insufficient to use as the data set for an assessment of heat transfer correlations of mixtures.

In this study, heat transfer coefficients in nucleate boiling are measured for single-, two- and three-component fluids over the whole range of their composition. Based on the measured data, heat transfer reduction in mixtures is made clear and an assessment of correlations is done to validate which type of correlations will be applicable to more than three-component mixtures.

2. Experimental method

Fig. 1(a) shows the boiling vessel held in a well-insulated temperature-controlled air-bath. The vessel is a vertical hollow cylinder of stainless steel, 110 mm ID and 600 mm high. Boiling takes place on the top surface

* Corresponding author. Tel.: +81-92-642-3471; fax: +81-92-641-9744.
E-mail address: fujita@mech.kyushu-u.ac.jp (Y. Fujita).

0017-9310/$ - see front matter © 2004 Elsevier Ltd. All rights reserved.
doi:10.1016/j.ijheatmasstransfer.2003.09.039

Nomenclature

a	thermal diffusivity (m^2/s)
C	coefficient in Eq. (1) (dimensionless)
D	departure bubble diameter (m)
g	gravitational acceleration (m/s^2)
h_{fg}	differential latent heat of evaporation (J/kg)
n	exponent in Eq. (1) (dimensionless)
K	influencing factor in Eq. (8) (dimensionless)
M	molecular weight (kg/kmol)
P	pressure (Pa)
P_c	critical pressure (Pa)
q	heat flux (W/m^2)
R_p	surface roughness (μm)
T	temperature (K)
T_c	critical temperature (K)
T_d	dew point temperature (K)
T_b	saturation or bubble point temperature (K)
T_w	heating surface temperature (K)
X	mole fraction in liquid (dimensionless)
Y	mole fraction in vapor (dimensionless)

Greek symbols

α	heat transfer coefficient (W/m^2 K)
α_{id}	ideal heat transfer coefficient defined in Eq. (10) (W/m^2 K)
β	mass transfer coefficient in liquid (m/s)
ΔT_{id}	ideal heating surface superheat defined in Eq. (9) (K)
ΔT_s	heating surface superheat $= T_w - T_b$(K)
T_{bp}	boiling range $= T_d - T_b$(K)
λ	thermal conductivity (W/mK)
v	kinematic viscosity (m^2/s)
θ	contact angle (deg)
ρ	density (kg/m^3)
σ	surface tension (N/m)

Subscripts

i	component-i; $i = 1$ for the more-, 2 for the moderate- and 3 for the less-volatile component
id	ideal
l	liquid
v	vapor

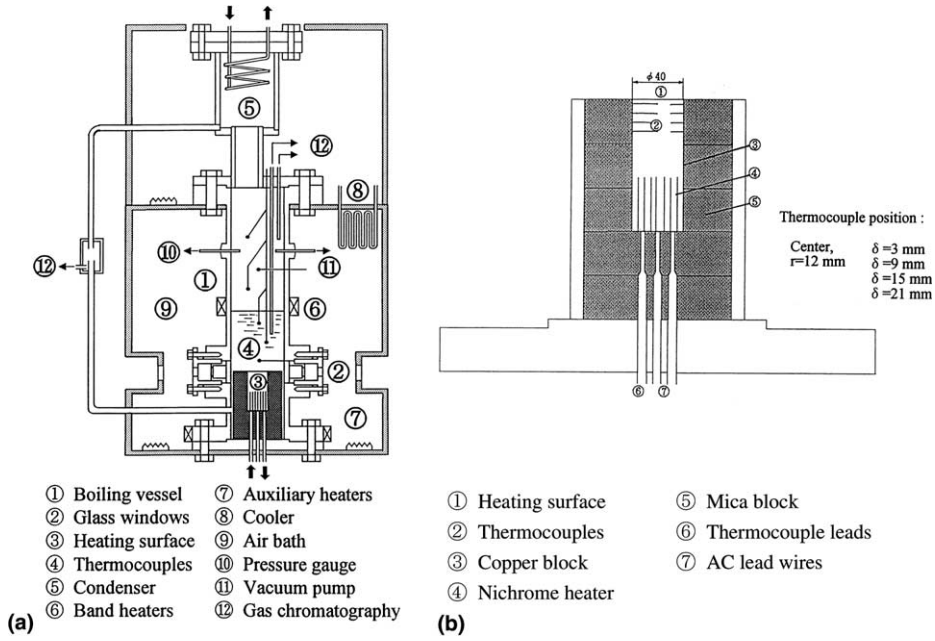

Fig. 1. Experimental apparatus. (a) Boiling vessel in an isothermal air-bath. (b) Heating surface block.

of cylindrical copper block shown in Fig. 1(b), which is fitted to the vessel. The copper cylinder is 40 mm in diameter and heated by nickel–chrome heaters inserted in slits of its base. As indicated in Fig. 1(b), eight thermo-

couples were placed at the center axis and 12 mm apart radial location of the cylinder and at four different depths from the top boiling surface. Temperatures measured on the centerline coincided each other with those measured at a radius of 12 mm within measurement errors, confirming uniform temperature in the radial direction and negligible heat loss from the cylindrical surface. Measured temperatures on the centerline are extrapolated to determine the boiling surface temperature and heat flux assuming one-dimensional conduction. Three thermocouples in bulk liquid and two thermocouples in the vapor space were installed. Their readings are monitored to confirm the boiling system operating at the saturation conditions. In case of mixture boiling in particular, measured compositions of liquid and vapor and their temperatures are plotted on the phase diagram to check the liquid and vapor in the boiling vessel lying on the boiling point and dew point curves respectively.

In advance of each series of measurement, the boiling surface was polished with a No. 0/4 emery paper, resulting in a surface roughness of 0.125 μm on average. Such a careful preparation of the surface contributed to well repeatable boiling data even when mixture compositions were widely changed in the present experiment.

Three refrigerants, R-134a (saturation temperature is 21.55 °C for an experimental pressure of 0.6 MPa), R-142b (45.11 °C), and R-123 (88.24 °C) were selected as pure components in the present experiment to comprise respectively the more-, moderate- and less-volatile component in case of three-component mixtures. This combination was determined in consideration that the level of saturation temperature and pressure is moderate in performing many measurement runs smoothly, the difference in saturation temperatures of three components is reasonably large (21.55, 45.11 and 88.24 °C), and the phase diagrams and physical properties of their two- or three-component mixtures are available or easily predictable from conventional methods. These refrigerants are also free from fouling of the boiling surface.

Table 1 compares for the present pure component fluids the chemical formula, the critical pressure and temperature, and several properties at the saturation temperature corresponding to the experimental pressure of 0.6 MPa.

To prepare mixture at desired compositions, pure component fluids were mixed on a weight base and then supplied to the degassed boiling vessel. A short time of degassing was repeated during heating up the mixture in the vessel to its saturation temperature. Power input to band heaters, auxiliary heaters in the air-bath and the boiling surface was carefully controlled in this process. Thereafter boiling experiment was begun in a closed system so that generated vapor from the heating surface was cooled in the condenser and the condensate returned to the liquid bulk through a return tube.

A small amount of bulk liquid in the boiling vessel and condensate in the return tube was respectively sampled time to time during boiling experiment to measure accurate liquid and vapor compositions by gas chromatography. Measure compositions of bulk liquid were found to agree within an accuracy of ±0.01 mole fraction with the prepared composition on a weight base. Thus, measured mole fractions of bulk liquid are used in the present paper to express the mixture composition. Thus their values are not always round number.

3. Data presentation

Total number of data points on boiling curves amounts to 1003 in the present experiment. It includes 113 points for three pure refrigerants, 558 points for

Table 1
A comparison of properties for three pure fluids

Property	Unit	R-134a	R-142b	R-123
Chemical formula	–	CH_2FCF_3	CH_3CClF_2	$CHCl_2CF_3$
Molecular weight	kg/kmol	102.03	100.50	152.93
Critical pressure	MPa	4.065	4.040	3.666
Critical temperature	°C	101.27	137.11	183.71
Properties for the saturation state at 0.6 MPa				
Saturation temperature	°C	21.55	45.11	88.24
Liquid density	kg/m^3	1218	1058	1307
Vapor density	kg/m^3	28.82	26.29	35.65
Heat of evaporation	kJ/kg	180.7	189.4	140.6
Liquid specific heat	kJ/kg K	1.422	1.325	1.109
Liquid thermal conductivity	W/mK	0.0830	0.0764	0.0583
Liquid kinematic viscosity	m^2/s	1.73×10^{-7}	2.54×10^{-7}	1.71×10^{-7}
Liquid Prandtl number	–	3.60	4.66	4.25
Surface tension	N/m	8.39×10^{-3}	8.98×10^{-3}	8.03×10^{-3}

25 compositions of two-component mixtures, and 332 points for 31 compositions of three-component mixture.

All the compositions for which heat transfer coefficients were measured are plotted on an equilateral composition triangle of Fig. 2, where three vertices indicate each mixture component, three sides stand for two-component mixtures and the inside denotes three-component mixtures. As clear from Fig. 2, boiling curves were obtained for mixture compositions rather evenly distributed on the composition triangle.

Boiling curves were obtained for a wide range of heat flux from onset point of boiling to a close point to critical heat flux in the both direction of increasing heat flux and decreasing heat flux, while an appreciable hysteresis was not observed on two boiling curves. Except for a few data points on boiling curve at low heat fluxes, boiling data for each composition are found to lay in the fully developed nucleate boiling regime. Thus heat transfer coefficient, α in W/(m^2 K), defined using either the wall temperature minus saturation temperature for pure fluids or the wall temperature minus bubble point temperature for mixtures is successfully expressed irrespectively of pure fluids and their mixtures by an exponential function of heat flux, q in W/m^2, as follows.

$$\alpha = Cq^n \tag{1}$$

To generalize all the data set measured in the present experiment, values of C and n in Eq. (1) were determined by fitting Eq. (1) to the data for every composition.

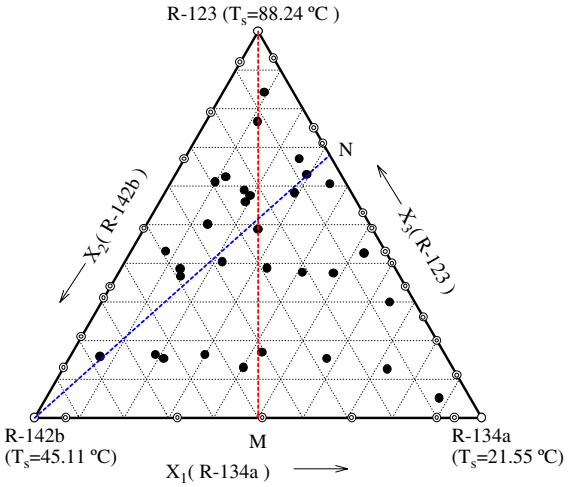

Fig. 2. Compositions where heat transfer measured.

Their values are compiled in Table 2, where the number of data points, heat flux range and the average error deviating from Eq. (1) are also given for reference. Note in the table that the suffix "1", "2", and "3" refers to the more-, moderate-, and less-volatile component in the present three fluids, respectively. Thus, "1" refers to R-134a, "2" to R-142b, and "3" to R-123. In case of two-component mixtures the smaller number of suffix refers to the more-volatile component and the larger number

Table 2
Coefficient C and exponent n in $\alpha = Cq^n$ to reproduce the measured heat transfer coefficients

X_1	X_2	X_3	C	n	Points	Heat flux (kW/m^2)	Error
1	0	0	1.21	0.83	38	4.7–458	3.2
0	1	0	1.76	0.79	40	6.3–404	3.9
0	0	1	1.86	0.77	35	4.7–378	2.3
0.07	0.93	0	1.53	0.79	37	9.3–377	4.1
0.32	0.68	0	0.96	0.81	23	12–377	4.2
0.51	0.49	0	0.87	0.81	22	12–386	4.4
0.71	0.29	0	0.74	0.84	24	11–357	4.3
0.90	0.10	0	1.70	0.79	23	9.7–388	3.0
0.94	0.06	0	0.96	0.84	13	8.2–386	0.8
0.07	0	0.93	0.89	0.78	26	11–378	2.8
0.25	0	0.75	1.44	0.71	27	15–370	1.3
0.29	0	0.71	1.52	0.71	19	18–456	2.0
0.47	0	0.53	1.31	0.70	21	29–365	3.9
0.51	0	0.49	0.76	0.74	31	31–391	3.6
0.57	0	0.43	1.54	0.68	26	47–362	2.3
0.60	0	0.4	1.68	0.67	15	44–465	2.0
0.66	0	0.34	13.03	0.51	18	25–328	2.1
0.74	0	0.26	13.71	0.51	21	15–263	2.8
0.80	0	0.20	8.05	0.57	23	15–211	2.6
0.89	0	0.11	11.28	0.57	24	6.2–259	3.6
0	0.08	0.92	0.61	0.82	17	12–364	1.3
0	0.21	0.79	0.61	0.80	23	13–369	2.3
0	0.33	0.67	0.44	0.83	22	11–371	2.7
0	0.51	0.49	0.67	0.79	25	18–389	2.5

Table 2 (*continued*)

X_1	X_2	X_3	C	n	Points	Heat flux (kW/m^2)	Error
0	0.66	0.34	0.33	0.85	18	19–255	4.7
0	0.69	0.31	0.25	0.88	19	7.3–247	1.9
0	0.79	0.21	0.37	0.86	18	16–217	1.1
0	0.87	0.13	1.23	0.77	23	15–289	2.2
0.07	0.77	0.07	0.99	0.76	10	20–353	4.2
0.08	0.49	0.08	0.74	0.77	11	18–360	1.1
0.09	0.07	0.09	1.78	0.70	11	18–371	0.8
0.10	0.29	0.10	1.46	0.72	12	11–376	0.5
0.11	0.12	0.11	1.30	0.72	12	18–429	0.7
0.12	0.26	0.12	1.02	0.74	12	13–374	0.7
0.13	0.48	0.13	1.64	0.71	11	11–265	4.1
0.14	0.36	0.14	1.02	0.74	12	13–351	1.8
0.14	0.49	0.14	1.21	0.73	12	14–358	2.5
0.17	0.24	0.17	0.45	0.80	9	21–338	1.5
0.19	0.25	0.19	0.79	0.76	11	20–408	2.1
0.19	0.65	0.19	3.09	0.66	11	16–257	2.4
0.20	0.23	0.20	1.16	0.73	11	17–331	1.3
0.21	0.64	0.21	2.79	0.66	10	14–353	4.1
0.22	0.38	0.22	1.21	0.72	11	17–367	2.9
0.26	0.07	0.26	0.95	0.73	10	29–345	0.6
0.26	0.25	0.26	0.50	0.79	10	28–365	2.2
0.29	0.08	0.29	0.50	0.78	10	27–377	0.8
0.29	0.13	0.29	0.66	0.76	10	28–331	1.6
0.30	0.54	0.30	4.27	0.63	12	16–377	3.2
0.33	0.28	0.33	1.63	0.69	10	27–376	2.2
0.36	0.04	0.36	0.60	0.77	10	27–350	1.6
0.40	0.47	0.40	9.18	0.56	11	6.3–340	4.5
0.41	0.21	0.41	1.62	0.68	9	40–365	2.2
0.42	0.41	0.42	9.82	0.55	14	8.3–372	2.4
0.48	0.14	0.48	4.02	0.61	10	30–378	1.5
0.52	0.05	0.52	2.15	0.66	9	41–357	2.2
0.58	0.27	0.58	16.00	0.51	9	14–293	1.8
0.64	0.06	0.64	11.00	0.53	11	18–368	2.3
0.73	0.15	0.73	16.90	0.51	11	4.9–303	1.6
0.88	0.07	0.88	7.92	0.59	10	4.9–185	2.9

Here, heat transfer coefficient α in W/m^2 K and heat flux q in W/m^2.

to the less-volatile component. Mixture composition is expressed in terms of mole fraction, such as X_1, X_2, and X_3 in liquid and Y_1, Y_2, and Y_3 in vapor. Eq. (1) with use of constants in Table 2 reproduces the measured heat transfer coefficients with an average deviation of 4.7% at most.

4. Results and discussions

4.1. Pure fluids

To confirm the validity of experimental apparatus and method used in the present experiment, measured heat transfer coefficients for pure fluids were compared in Fig. 3 with two typical correlations, Stephan and Abdelsalam dimensionless correlation [17] derived from a regression analysis of many data and Nishikawa et al. dimensional correlation [18] derived from thermodynamic similarity of thermophysical properties, which are respectively expressed as follows

$$\frac{\alpha d}{\lambda_l} = 207\left(\frac{qd}{\lambda_l}\right)^{0.745}\left(\frac{\rho_v}{\rho_l}\right)^{0.581}\left(\frac{v_l}{a_l}\right)^{0.533} \tag{2}$$

$$d = 0.0146\theta\sqrt{2\sigma/g(\rho_l - \rho_v)}, \quad \theta = 35^\circ \tag{3}$$

and

$$\alpha = \frac{31.4P_c^{1/5}}{M^{1/10}T_c^{9/10}}(8R_p)^{0.2(1-P/P_c)} \times \frac{(P/P_c)^{0.23}q^{4/5}}{[1-0.99(P/P_c)]^{0.9}} \tag{4}$$

$$R_p = 0.125\ \mu\text{m} \tag{5}$$

Quite a close agreement of the data with the predictions was obtained for respective three pure fluids. Thus the present experimental apparatus and method were concluded as appropriate for mixture experiment,

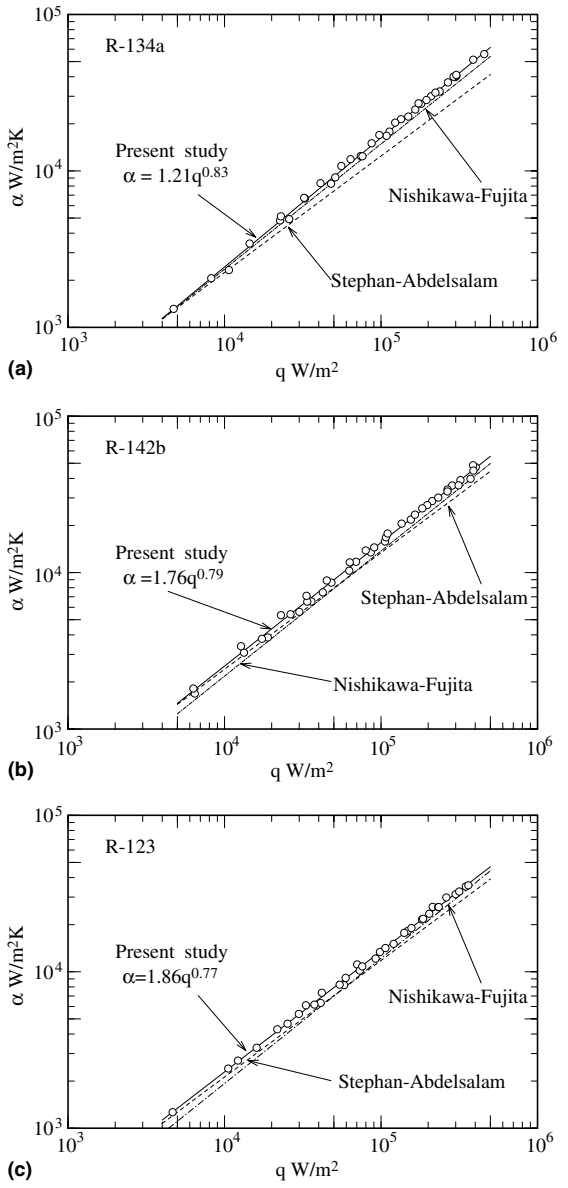

Fig. 3. Heat transfer coefficient for three pure fluids. (a) R-134a, (b) R-142b, (c) R-123.

providing reliable mixture data to analyze the composition dependency of heat transfer coefficient in the following sections.

4.2. Two-component mixtures

Boiling curves for two-component mixtures were obtained for the marked points on the three sides of the triangle shown in Fig. 2. Boiling curves of the mixtures, although not shown here, are found to shift to the right hand side, indicating the reduction of heat transfer compared to pure fluids. To show more clearly the heat transfer reduction depending on mixture composition, heat transfer coefficients are plotted against the mole fraction of the more-volatile component with three heat fluxes as parameter in Fig. 4. Top figures of Fig. 4 illustrate the phase diagrams determined from the modified BWR equation of state [19] and the plotted data on them indicate the mole fractions in vapor and liquid that were measured for sampled condensate and bulk liquid during boiling experiments. Among three mixtures the boiling range, i.e., the dew point minus bubble point temperature, is largest for R-134a (X_1) and R-123 (X_3) mixture and smallest for R-134a (X_1) and R-142b (X_2) mixture.

It is clear from a comparison of the three bottom figures of Fig. 4 that heat transfer coefficients are reduced substantially in the order of an increasing boiling range. Thus the reduction is most significant in R-134a (X_1) and R-123 (X_3) mixture compared to R-134a (X_1) and R-142b (X_2) mixture. Even for the same mixture composition, heat transfer reduction is not uniform for heat flux variations, with larger reductions occurring at higher heat fluxes. These two characteristics regarding the influence of boiling range and heat flux on heat transfer reduction were also observed more or less in other kinds of two-component mixtures investigated in the past.

4.3. Three-component mixtures

Heat transfer coefficient of three-component mixtures varies as a function of the mixture composition and heat flux as expressed in Eq. (6), while the mole fraction of each component satisfies Eq. (7). Hence one variable is deleted from Eq. (6) but three are still remaining, which requires three-dimensional presentation of heat transfer coefficient. To avoid such stereoscopic figures, two-dimensional presentation is used hereafter either with heat flux as parameter or with putting some constraint on the mixture compositions.

$$\alpha = F(X_1, X_2, X_3, q) \tag{6}$$

$$X_1 + X_2 + X_3 = 1 \tag{7}$$

Fig. 5 shows typical results indicating the reduction of heat transfer coefficient of three-component mixtures where the mole fraction of R-123 (X_3) is varied with the mole fractions of other two-components being kept equal, i.e., $X_1 = X_2$. Thus Fig. 5(a) denotes boiling curves and Fig. 5(b) shows the variation of heat transfer coefficient, respectively along the perpendicular line from M on the base to the vertex for R-123 on the composition triangle of Fig. 2. In Fig. 5(b), thus, the left end of the abscissa refers to two-component mixture of R-134a ($X_1 = 0.5$) and R-142b ($X_2 = 0.5$) and the right end indicates pure fluid of R-123 ($X_3 = 1$). Dotted curves

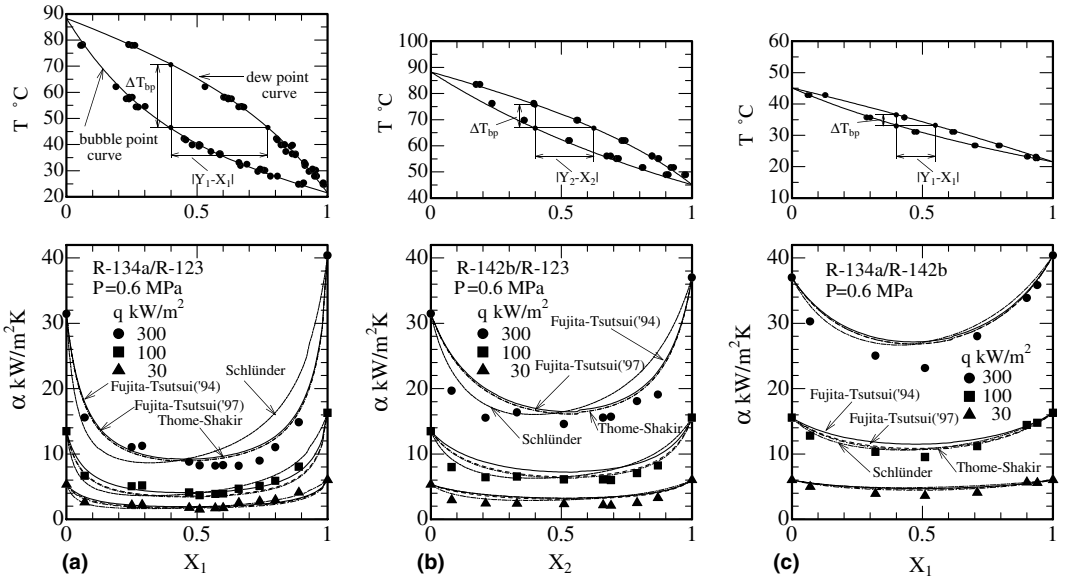

Fig. 4. Heat transfer coefficient for two component mixtures. (a) R-134a (X_1) and R-123 (X_3), (b) R-142b (X_2) and R-123 (X_3), (c) R-134a (X_1) and R-142b (X_2).

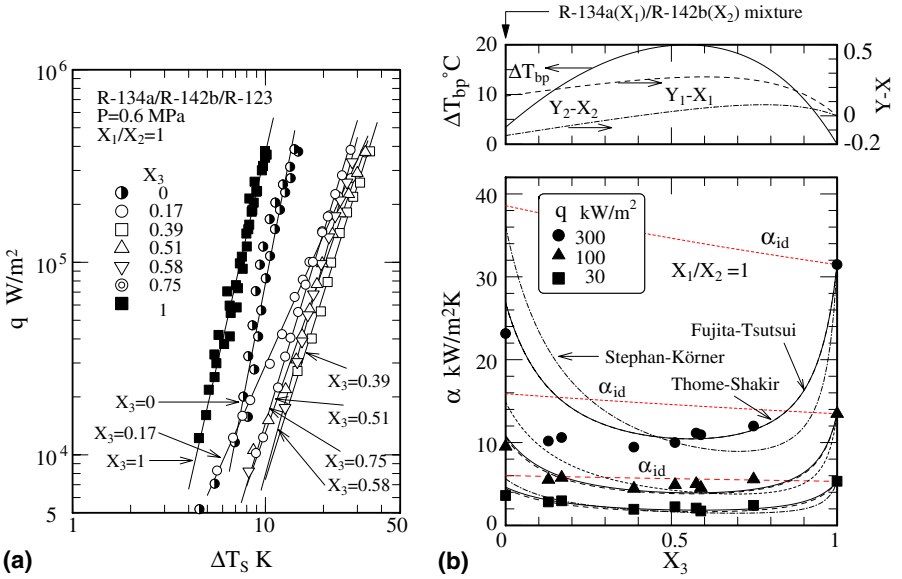

Fig. 5. Heat transfer coefficient for three-component mixtures (X_3 is varied with keeping $X_1/X_2 = 1.0$). (a) Boiling curves, (b) heat transfer coefficient.

in Fig. 5(b) indicate the ideal heat transfer coefficient calculated from Eq. (10) mentioned in the later section. Compared with the ideal coefficient, heat transfer coefficient of mixture is substantially reduced, with the larger reduction at higher heat fluxes. Top figure of Fig. 5(b) indicates the boiling range and the composition difference between vapor and liquid for reference. A larger reduction of heat transfer coefficient is occurring at concentrations where the boiling range is large.

Fig. 6 shows another result for the variation of heat transfer coefficient with the mixture composition. The concentration of R-123 (X_2) is varied with keeping

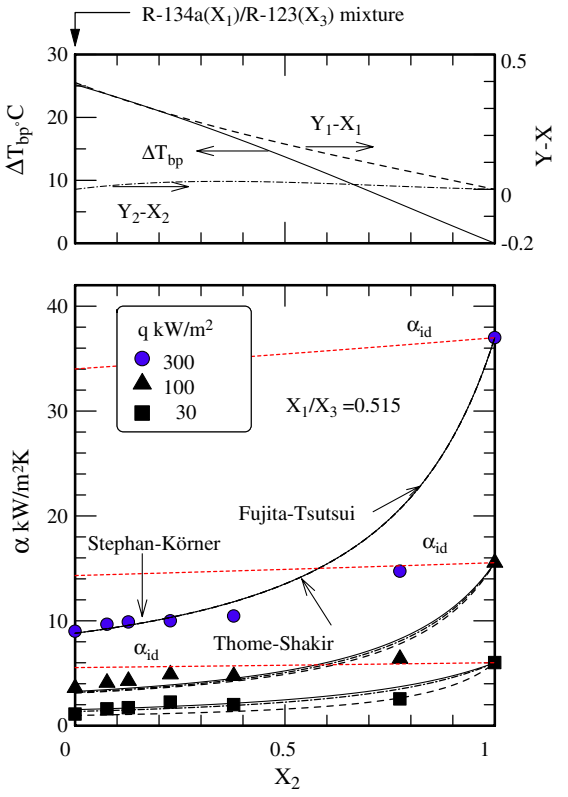

Fig. 6. Heat transfer coefficient for three-component mixtures (X_2 is varied with keeping $X_1/X_3 = 0.515$).

$X_1/X_3 = 0.515$, thus along the line from N on the oblique side to the vertex for R-142b on the composition triangle shown in Fig. 2. Thus the left end of the abscissa of Fig. 6 denotes two-component mixture of R-134a ($X_1 = 0.34$) and R-123 ($X_3 = 0.66$), and the right end refers to pure fluid of R-142b ($X_2 = 1.0$). Differently to the concentration dependency observed in Fig. 5(b), heat transfer coefficient varies monotonously in this case. However this variation is reasonable since heat transfer coefficient is more reduced as the boiling range becomes larger.

To overview heat transfer reduction over the whole composition range of three-component mixtures, contour maps of heat transfer coefficient are shown for a heat flux of 300 kW/m^2 in Fig. 7(a) and for 100 kW/m^2 in Fig. 7(b). Similar patterns of maps are obtained for other heat fluxes, while not shown here. It is found from Fig. 7 that heat transfer coefficient is highly reduced in the composition range close to two-component mixture of R-134a (X_1) and R-123 (X_3) of nearly equal moles. This result is expected from Fig. 4 because the two-component mixture of R-134a (X_1) and R-123 (X_3) gives the lowest heat transfer coefficients compared to the other two two-component mixtures.

4.4. Phase diagram of three-component mixtures

Fig. 8 illustrates the phase diagram of three-component mixture where L(1), M(2) and H(3) refer to the more-, moderate- and less-volatile components, respectively. As seen there the dew point forms a convex surface extending in the upward direction, while the bubble point forms a concave surface. These two surfaces intersect with an isothermal plane of given temperature to determine the bubble point isothermal line L′–L″ and the dew point isothermal line V′–V″. Thus each liquid state (L) on the bubble point isotherm of a composition of (X_1, X_2, X_3) is at equilibrium with the vapor state (V) on the dew point isotherm of a corresponding composition of (Y_1, Y_2, Y_3).

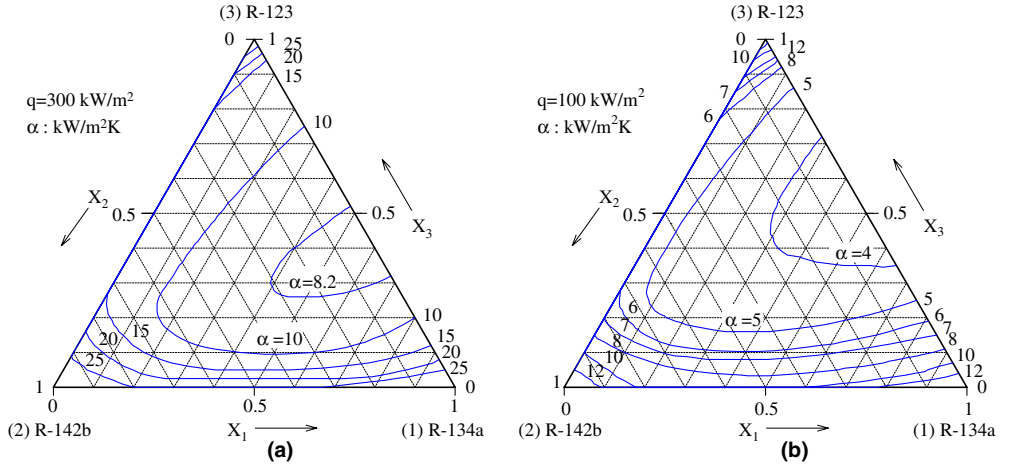

Fig. 7. Contour of heat transfer coefficient for three-component mixtures. (a) $q = 300$ kW/m^2, (b) $q = 100$ kW/m^2.

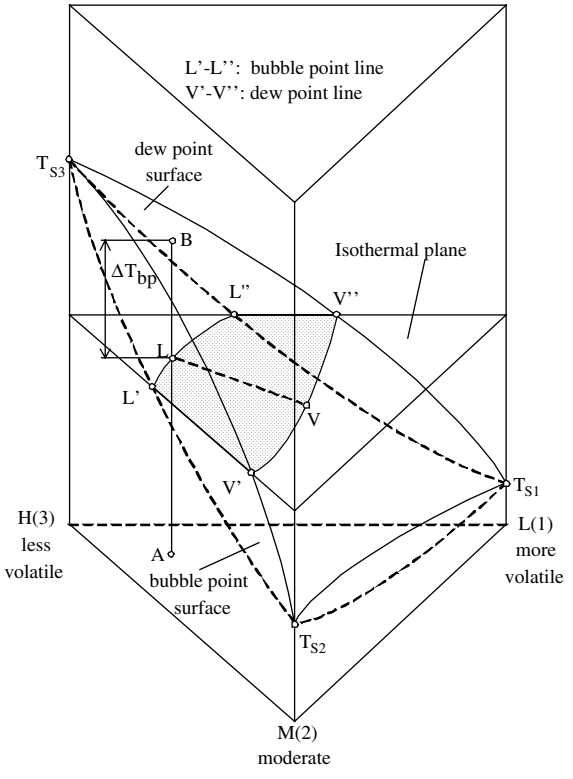

Fig. 8. Phase equilibrium diagram for three-component mixtures.

Fig. 9 shows as an example the equilibrium liquid and vapor lines at 50 °C for the present three-component mixtures. Three liquid points denoted on an isothermal bubble point line for 50 °C are equilibrium with the corresponding vapor points on the isothermal dew point line as indicated by the lines with arrow heads.

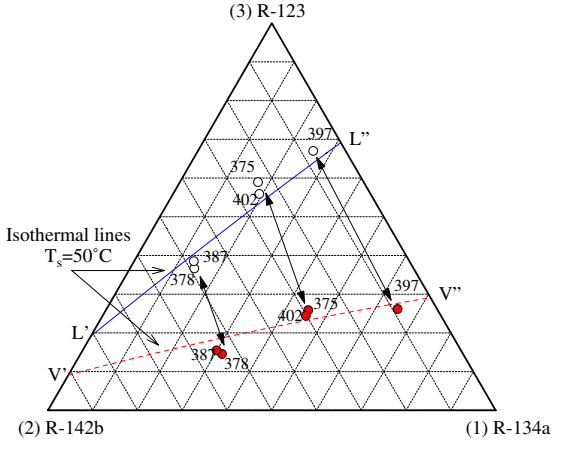

Fig. 9. Bubble point and dew point lines in equilibrium at 50 °C.

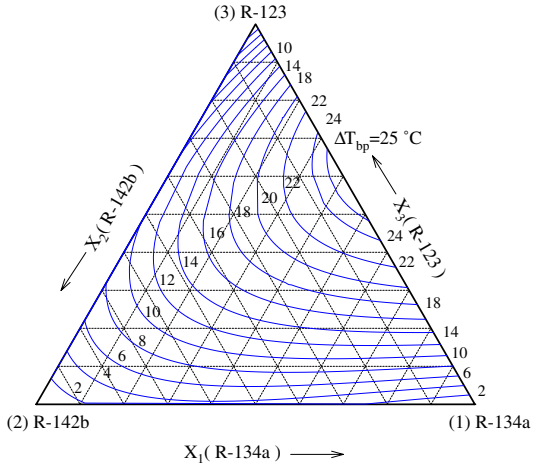

Fig. 10. Contour of the boiling range for three-component mixtures.

Plotted data indicate the measured compositions of the sampled bulk liquid and condensate during boiling experiments.

For a given liquid composition of (X_1, X_2, X_3) on the composition triangle shown in Fig. 8, a vertical line segment L–B between the bubble point and dew point surfaces determines the boiling range ΔT_{bp}. Thus the boiling range becomes a unique function of mixture composition and Fig. 10 shows a contour map of the boiling range for the present mixtures.

4.5. Assessment and recommended correlations for three-component mixtures

Heat transfer correlations for mixtures [4,8–10,12–14] that will be compared with the present mixture data are all reduced to the form of Eq. (8) and listed in the chronological order in Table 3.

$$\frac{\alpha}{\alpha_{id}} = \frac{1}{1+K} \tag{8}$$

Here α_{id} is the ideal heat transfer coefficient defined using an ideal wall superheat, ΔT_{id}, that is determined as a molar interpolation of the wall superheats for mixture components evaluated at the same heat flux as the mixture. Thus,

$$\Delta T_{id} = \sum (X_i \Delta T_{si}) \tag{9}$$

$$\alpha_{id} = \frac{q}{\Delta T_{id}} = \frac{1}{\sum (X_i/\alpha_i)} \tag{10}$$

At first all the correlations in Table 3 were compared with the data for two-component mixtures to sort several correlations that reproduced the data with small prediction errors. In Fig. 4, four best correlations sorted

Table 3
K factor in typical correlations for mixtures, $\alpha/\alpha_{id} = 1(1+K)$

Authors	K
Stephan–Kömer [4]	$A_0\lvert Y-X\rvert(0.88+0.12P)$ P in bar
Jungnickel et al. [8]	$K_0\lvert Y-X\rvert\left(\frac{\rho_v}{\rho_l}\right)q^{(0.48+0.1X_1)}$ q in W/m^2
Schlünder [9]	$\frac{\Delta T_s\lvert Y-X\rvert}{\Delta T_{id}}\left[1-\exp\left(\frac{-B_0 q}{\beta_l\rho_l h_{fg}}\right)\right]$ $B_0=1.0$, $\beta_l=(1\text{–}3)\times10^{-4}$ m/s
Thome [10]	$\frac{\Delta T_{bp}}{\Delta T_{id}}$
Thome–Shakir [12]	$\frac{\Delta T_{bp}}{\Delta T_{id}}\left[1-\exp\left(\frac{-B_0 q}{\beta_l\rho_l h_{fg}}\right)\right]$ $B_0=1.0$, $\beta_l=(2)\times10^{-4}$ m/s
Fujita–Tsutsui [13]	$\frac{\Delta T_{bp}}{\Delta T_{id}}\left[1-0.8\exp\left(\frac{-q}{10^5}\right)\right]$ q in W/m^2
Fujita–Tsutsui [14]	$\frac{\Delta T_{bp}}{\Delta T_{id}}\left\{1-\exp\left[\frac{-60q}{\rho_v h_{fg}}\left(\frac{\rho_v^2}{\sigma g(\rho_l-\rho_v)}\right)^{1/4}\right]\right\}$

in this way are compared with the data, with the other correlations deleted to avoid confusion. Thom and Shakir correlation [12] and two Fujita and Tsutsui correlations [13,14] are found to reproduce the data for two-component mixtures rather well over the whole mole fraction range. Schlünder correlation [9] indicated also the same order of errors. But a close examination found Schlünder correlation to either underestimate or overestimate heat transfer coefficient depending on the range of mixture concentration. The deviations in the opposite directions canceled with each other to result in a small average prediction error.

Sorted correlations using two-component mixture data commonly include the boiling range as parameter. This result surmises that heat transfer coefficient will be more reduced at mixture compositions where the boiling range becomes larger. To check this surmise the boiling range shown as a contour map in Fig. 10 is compared with the contours of heat transfer coefficients shown in Fig. 7. Clearly there is observed similarity between the compared contour patterns. Thus as validated for two-component mixtures the boiling range is likely a key parameter to account for heat transfer reduction in three-component mixtures too.

In Figs. 5(b) and 6, the predicted heat transfer coefficients using Thome and Shakir correlation [12] and Fujita and Tsutsui correlation [14] are shown for a comparison with the data. As expected, these two correlations are found to successfully reproduce the data for three-component mixtures too.

Stephan and Körner [4] and Stephan and Presser [7] employed the concentration difference between the vapor and liquid at equilibrium as a key parameter in developing their correlations of two-component mixtures. They claimed their correlations are applicable to three-component mixtures by replacing K-factor in Eq. (8) as follows.

$$K = K_{13}|Y_1 - X_1| + K_{23}|Y_2 - X_2| \tag{11}$$

Here K_{13} and K_{23} are K-factors for two-component mixtures. In applying this type of correlations, however, the phase equilibrium calculation is needed in the first place to determine the vapor composition (Y_1, Y_2, Y_3) in equilibrium with the bulk liquid of a given composition (X_1, X_2, X_3) as exemplified in Fig. 9. Another problem in using Eq. (11) arises, as pointed out by Stephan and Preusser [7], that each factor K_{ij} determined for two-component mixtures should be more or less reduced when applied to three- or more than three-component mixtures. Otherwise heat transfer coefficient would be highly underestimated. However there is no general means to modify the values of K_{ij} when applied to more than two-component mixtures.

Fig. 11 compares the predicted heat transfer coefficients (α_c) with all the measured coefficients (α_m) for three-component mixtures. Both correlations by Thome and Shakir [12] and by Fujita and Tsutsui [14] well reproduce the measured data within ± 25% accuracy lines. The root mean square error is evaluated as 19% in Thome and Shakir correlation and 17% in Fujita and Tsutsui correlation. When Stephan and Körner correlation [4] was applied to the same data set of three-component mixtures, the root mean square error was evaluated as 32%. In this case, values of K_{ij} in Eq. (11) were determined from the present two-component mixture data as $K_{13} = 8.19$ ($A_0 = 5.12$) for R-134a (X_1) and R-123 (X_3) mixture and $K_{23} = 7.68$ ($A_0 = 4.80$) for R-142b (X_2) and R-123 (X_3) mixture. These values were about three times larger than the value recommended by Stephan and Körner [4] but used without any modification in predicting heat transfer coefficients of three-

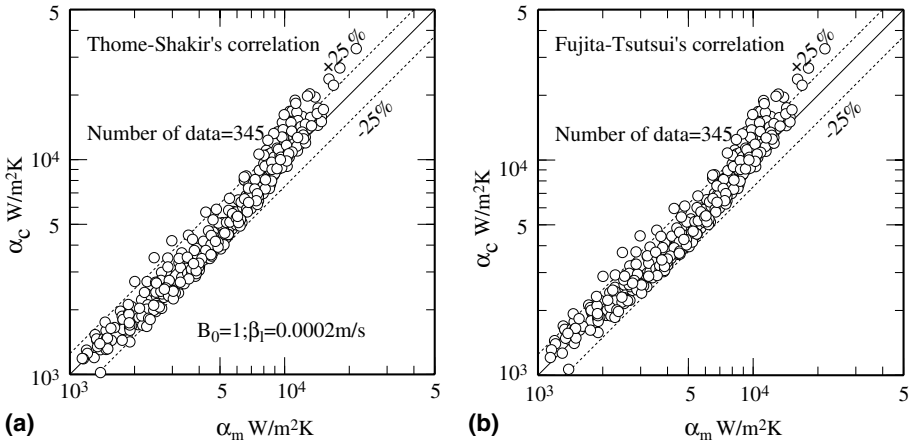

Fig. 11. Comparison of predictions with data for three-component mixtures. (a) Thome and Shakir correlation. (b) Fujita and Tsutsui correlation.

component mixtures. The prediction from Stephan and Körner correlation is also shown in Fig. 5(a) and Fig. 6. The deviation in the opposite directions as observed in Fig. 5(b) results in a larger root mean square error of 32%.

5. Conclusions

Heat transfer coefficients in nucleate boiling were measured for three-as well as two-component mixtures in the whole range of composition with refrigerants R-134a, R-142b and R-123 as comprising pure components. It was found that heat transfer coefficients of mixtures are reduced in a comparison with the ideal coefficients interpolated between pure components. Such a reduction becomes more significant as heat flux is increased. The boiling range is likely to be a key parameter to account for heat transfer reduction in boiling of mixture. This premise is supported by similarity between two contour maps of heat transfer coefficient and the boiling range. Correlations by Thome and Shakir and by Fujita and Tsutsui, which include the boiling range as parameter, succeeded in reproducing the present three-component mixture data as well as the two-component mixture data. These correlations are expected applicable to more than three-component mixtures in general.

References

[1] W.R. Van Wijk, A.S. Vos, S.J.D. Van Stralen, Heat transfer to boiling binary liquid mixtures, Chem. Eng. Sci. 5 (1956) 68–80.

[2] C.V. Sternling, L.J. Tichacek, Heat transfer coefficients for boiling mixtures—experimental data for binary mixtures of large relative volatility, Chem. Eng. Sci. 16 (1961) 297–337.

[3] M. Körner, Messungen des wärmeübergang bei der verdampfung binärer gemische, Wärme- und Stoffübertragung 2 (1969) 178–191.

[4] K. Stephan, M. Körner, Berechnung des warmeübergangs verdamppfender binärer flüssigkeitsgemische, Chemie. Ing. Techn. 41 (1969) 409–417.

[5] W.F. Calus, P. Rice, Pool boiling–binary liquid mixtures, Chem. Eng. Sci. 27 (1972) 1687–1697.

[6] J.R. Thome, Latent and sensible heat transfer rates in the boiling of binary mixtures, J. Heat Transfer 104 (1982) 474–478.

[7] K. Stephan, P. Preusser, Heat transfer and critical heat flux in pool boiling of binary and ternary mixtures, Ger. Chem. Eng. 2 (1979) 161–169.

[8] H. Jungnickel, P. Wassilew, W.E. Kraus, Investigations on the heat transfer of boiling binary refrigerant mixtures, Int. J. Refrig. 3 (1980) 129–133.

[9] E.U. Schlünder, Über den wärmeübergang bei der blasenverdampfung von gemischen, Verfahrenstechnik 16 (1982) 692–698.

[10] J.R. Thome, Prediction of binary mixture boiling heat transfer coefficients using only phase equilibrium data, Int. J. Heat Mass Transfer 26 (1983) 965–974.

[11] H.C. Unal, Prediction of nucleate pool boiling heat transfer coefficients for binary mixtures, Int. J. Heat Mass Transfer 29 (1986) 637–640.

[12] J.R. Thome, S. Shakir, A new correlation for nucleate pool boiling of aqueous mixtures, AIChE Symp. Ser. 83, 1987, pp. 46–51.

[13] Y. Fujita, M. Tsutsui, Heat transfer in nucleate pool boiling of binary mixtures, Int. J. Heat Mass Transfer 37 (1994) 291–302.

[14] Y. Fujita, M. Tsutsui, Heat transfer in nucleate boiling of binary mixtures (development of a heat transfer correlation), JSME Int. J. Ser. B 40 (1997) 134–141.

[15] L.N. Grigor'ev, L.A. Sarkisyan, A.G. Usmanov, An experimental study of heat transfer in the boiling of three component mixtures, Int. Chem. Eng. 8 (1968) 76–78.
[16] S.M. Bajorek, J.R. Lloyd, J.R. Thome, Evaluation of multicomponent pool boiling heat transfer coefficients, in: Proc. 9th Int. Heat Transfer Conf., vol. 2, 1990, pp. 39–44.
[17] K. Stephan, M. Abdelsalam, Heat-transfer correlations for natural convection boiling, Int. J. Heat Mass Transfer 23 (1980) 73–87.
[18] K. Nishikawa, Y. Fujita, H. Ohta, S. Hidaka, Effect of the surface roughness on the nucleate boiling heat transfer over the wide range of pressure, in: Proc. 7th Int. Heat Transfer Conf., vol. 4, 1982, pp. 61–66.
[19] H. Nishiumi, S. Saito, An improved generalized BWR equation of state applicable to low reduced temperatures, J. Chem. Eng. Jpn. 8 (1975) 356–362.